Bending and Straightening of DNA Induced by the Same Ligand: Characterization with the Atomic Force Microscope†

Helen G. Hansma,*,‡ Kenneth A. Browne,§ Magdalena Bezanilla,‡ and Thomas C. Bruice§

Departments of Physics and Chemistry, University of California, Santa Barbara, California 93106

Received December 8, 1994; Revised Manuscript Received March 4, 1994®

ABSTRACT: A new ligand, MGT-6b, binds to DNA with two linked parts: a polyamine that binds to the phosphate backbone and a tripyrrole peptide that binds to the minor groove. This ligand decreases the curvature of bent kinetoplast DNA (kDNA) and also *increases* the curvature of a 400-bp DNA that is used as a molecular weight standard (M400), as characterized with the atomic force microscope (AFM). MGT-6b is more effective than distamycin at straightening kDNA. MGT-6b retards the electrophoretic mobility of M400 DNA, although neither of its two component parts alters the mobility of M400 or its curvature as seen in the AFM. Thus, both parts of the ligand are needed for the "vise grip" mode of binding that affects DNA bending. The ability of MGT-6b to both bend and straighten DNA is probably related to the very different DNA sequences and, hence, structures of kDNA and M400 DNA.

Bending and curving of DNA are important because of their role in many processes (Spolar & Record, 1994; vonHippel, 1994), including transcription (Perez-Martin & Espinosa, 1993; Rees et al., 1993), replication (Caddle et al., 1990; Gille et al., 1991), the excision of damaged nucleotides from DNA (Shi et al., 1992), and the packaging of DNA into nucleosomes (Allen et al., 1993; Griffith, 1975). We are investigating the bending and curving of DNA by using the atomic force microscope (AFM[1]) (Binnig et al., 1986; Rugar & Hansma, 1990) to characterize the conformations of DNA molecules that are naturally either bent or straight and the effect of small organic ligands on these conformations.

We have used two ligands, distamycin and microgonotropen-6b (MGT-6b). Distamycin is a natural antibiotic that has the ability to straighten abnormally bent kinetoplast DNA, the mitochondrial DNA from trypanosomes and related parasitic protozoa (Griffith et al., 1986; Wu & Crothers, 1984). A new ligand class called microgonotropens (MGTs) (He et al., 1993, 1994) is more stable than distamycin and better than distamycin at straightening kinetoplast DNA. The microgonotropen used in this work (MGT-6b) has two components: a tripyrrole peptide (**2**) (He et al., 1993; Wade & Dervan, 1987) that binds to the minor groove of DNA and a polyamine (tren) that binds to the phosphate backbone (Figure 1).

The AFM can image bare, uncoated DNA molecules on a flat surface at submolecular resolution by raster-scanning a sharp tip back and forth across the surface (Binnig et al., 1986; Rugar & Hansma, 1990). For imaging the short DNA molecules used in this research, it was necessary to use the tapping mode of AFM imaging (Hansma et al., 1993b; Zhong et al., 1993). In the tapping mode, the tip oscillates at high frequency, touching the sample surface only at the bottom of the oscillation, with the height changes on the sample surface being detected by changes in the amplitude of the oscillation. The lateral forces are basically eliminated, so that the DNA is not pushed by the tip. Measured DNA widths are typically 5–9 nm, which is unusually low for air-imaging (Hansma et al., 1992; Vesenka et al., 1992). [Measured widths in the AFM are typically wider than the expected widths of 2–3 nm due to the width of the imaging tip (Hansma & Hoh, 1994).] Another advantage of the tapping mode is that small DNA fragments can be imaged easily. Such small pieces of DNA are difficult to image in the AFM without the tapping mode. In propanol or butanol, which give the highest resolution AFM

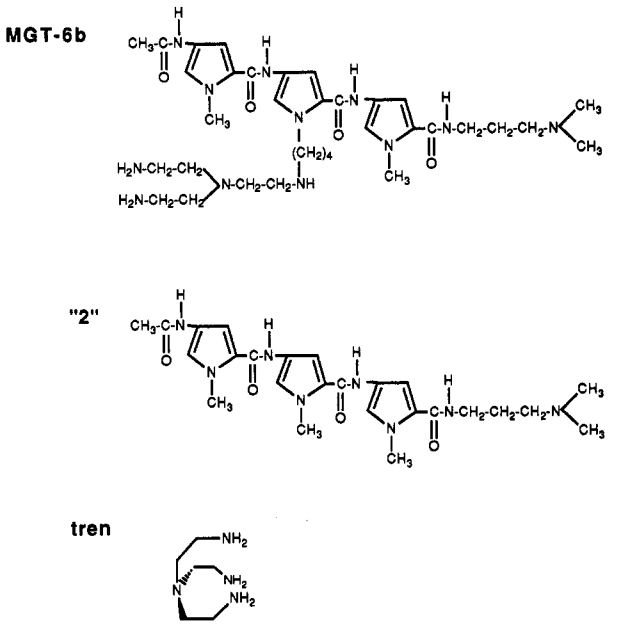

FIGURE 1: Structure of MGT-6b (He et al., 1994) and its two parts, **2** (He et al., 1993; Wade & Dervan, 1987) and tren. Distamycin resembles **2**, with the substitution of amidine for the carboxyl-terminal $CH_2N(CH_3)_2$ and a formyl group for the amino-terminal acetyl group of **2**.

† Supported by NSF DIR 9018846 and Digital Instruments (H.G.H. and M.B.) and by the Office of Naval Research N000 14-90-J-4132 (K.A.B. and T.C.B.).

* Author to whom correspondence should be addressed.

‡ Department of Physics.

§ Department of Chemistry.

® Abstract published in *Advance ACS Abstracts,* July 1, 1994.

[1] Abbreviations: AFM, atomic force microscope; bp, base pairs; kDNA, a highly bent segment of kinetoplast DNA; MGT, microgonotropen, a class of ligands containing two covalently linked parts, a tripyrrole peptide that binds to the minor groove of DNA and a polyamine that binds to the phosphate backbone; M400, 400-bp DNA sold as a molecular weight standard for gel electrophoresis; tren, tris(2-aminoethyl)amine; **2**, the tripyrrole peptide shown in Figure 1, which is the minor-groove-binding portion of MGT-6b.

0006-2960/94/0433-8436$04.50/0

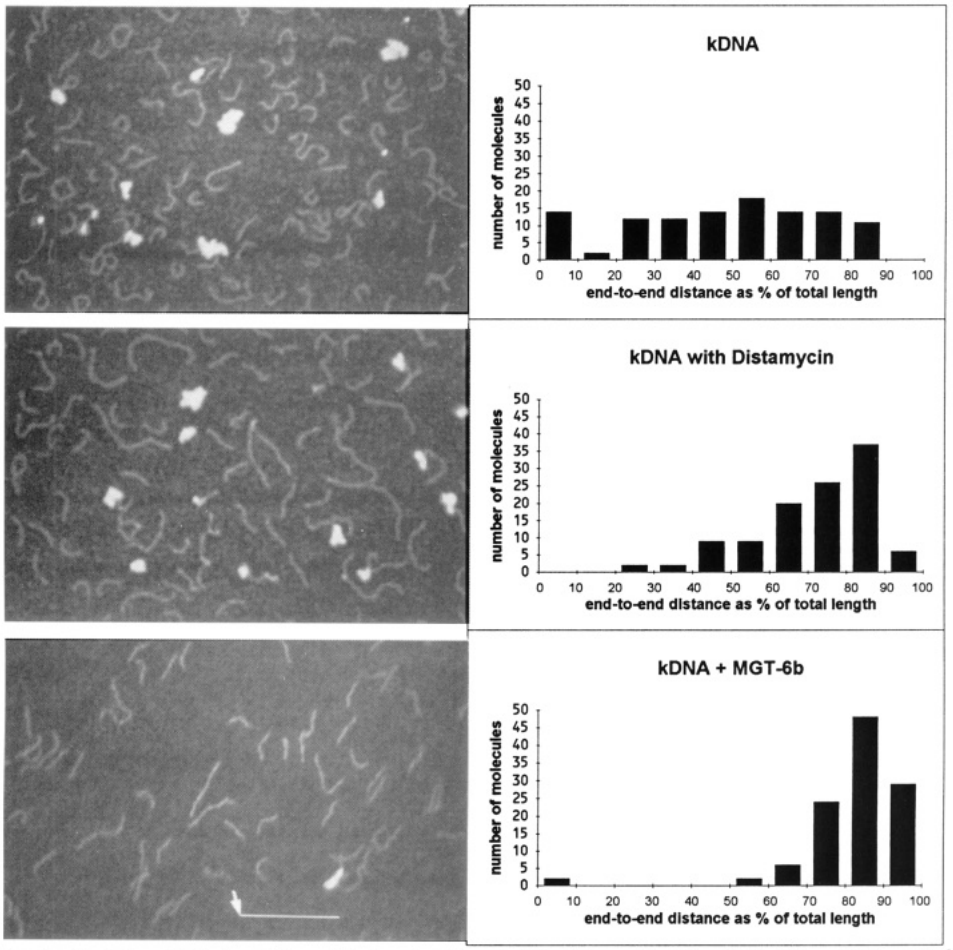

FIGURE 2: kDNA without added ligand (A, top left, and B, top right) and with distamycin (C, middle left, and D, middle right) or MGT-6b (E, bottom left, and F, bottom right) at a ratio of 1 ligand molecule/7 bp DNA. Atomic force microscopy in the tapping mode in dry helium (A, C, and E). Scale bar = 200 nm (arrow). Histograms of the end-to-end distances for 111 kDNA molecules (B, D, and F).

images of DNA (Hansma & Hansma, 1993; Hansma et al., 1992), small DNA molecules stick to the tip more easily than long DNA, which stays attached to mica better. In air or dry helium in the normal imaging mode, small DNAs do not stick to the tip, but the widths of DNA in air can be as large as 20 nm. Since a circle of 219-bp kDNA has a diameter of only 20 nm, these circles usually look like blobs in air in the normal imaging mode. In contrast, with the tapping mode, the circles are very clear (Figure 2A).

MATERIALS AND METHODS

Materials. Plasmid pPK201/CAT containing the highly bent segment of kinetoplast DNA from *Crithidia fasciculata* was provided by Paul T. Englund (Kitchin et al., 1986). A 219-bp fragment of kinetoplast DNA was digested from the plasmid with *Bam*HI (Kitchin et al., 1986) and purified by standard methods.

M400 DNA, a 400-bp DNA used as a molecular weight standard, was obtained from BioVentures, Inc. (Murfreesboro, TN), supplied at 10 mg/mL in water. Since the sequence of this DNA is proprietary, we know only the positions, sequences, and adjacent bases of runs containing three or more A's and/or T's.

The syntheses of **2** (He et al., 1993) and MGT-6b (He et al., 1994) have been described. Reagents obtained commercially include the following: tris(2-aminoethyl)amine (tren, Aldrich Chemical Co., Milwaukee, WI); ethidium bromide and *N*-(2-hydroxyethyl)piperazine-*N*′-2-ethanesulfonic acid (HEPES free acid, Sigma, St. Louis, MO); hydroxyethyl agarose (NuSieve 3:1, FMC, Rockland, ME). Distilled, deionized water was used for all biological reactions and dilutions.

Preparing Samples for AFM. DNA was incubated for 15 min at room temperature with the specified ligand in a buffer containing 20 mM HEPES and 5 mM $MgCl_2$, pH 7.6 (KOH). An aliquot of approximately 0.2 μL containing 500–800 pg of DNA was placed on fresh-split mica, rinsed for 30 s with MilliQ purified water, and dried with compressed air and in a desiccator over P_2O_5 for several hours before imaging in the AFM. By counting the number of molecules per field, we estimate that on the order of 50% of the applied DNA is bound to the mica substrate.

Atomic Force Microscopy (AFM). Samples were imaged in a Nanoscope III with multimode AFM (Digital Instruments, Santa Barbara, CA) in the tapping mode (Hansma et al., 1993b; Zhong et al., 1993) at a scan rate of 3–5 Hz in dry helium. Cantilevers were 120-μm-long silicon NanoProbes with resonant frequencies of 300–420 kHz.

For accurate measurements, it is important to scan until drift and creep have dropped to low levels. The extent of drift and creep can be measured by comparing distances between the same features on images captured from successive "up" and "down" traces. Measurements that agreed to within 10% were considered adequate.

Linear DNA molecules, especially at high concentrations, often joined end-to-end in structures 2 or more times as long as single molecules. The white patches in some images are due to the HEPES–Mg buffer. These patches can be removed

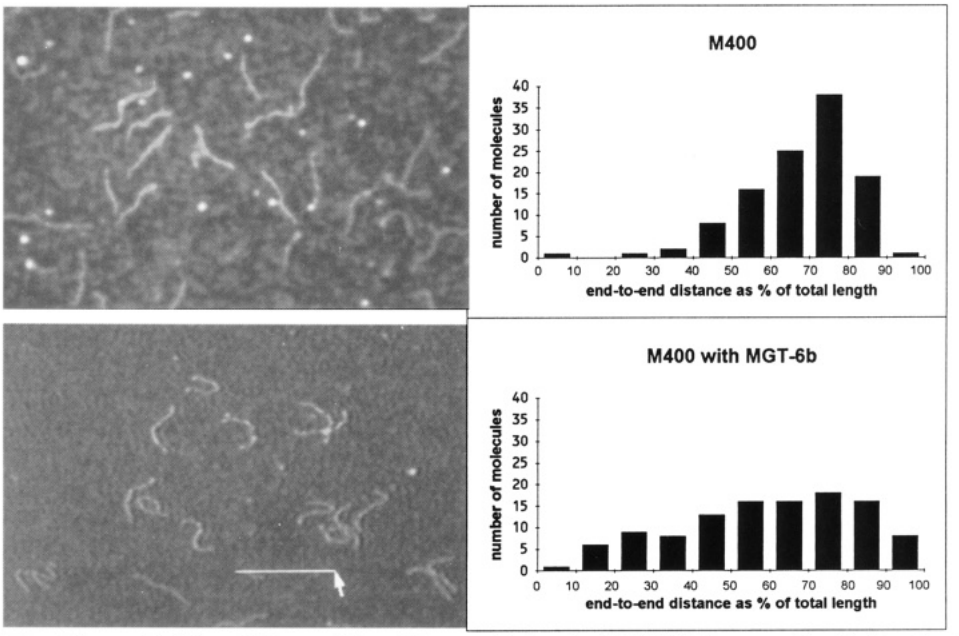

FIGURE 3: M400 DNA without added ligand (A, top left, and B, top right) and with MGT-6b at a ratio of 1 ligand molecule/1.4 bp DNA (C, bottom left, and D, bottom right). Atomic force microscopy in the tapping mode in dry helium (A and C). Scale bar = 200 nm (arrow). Histograms of the end-to-end distances for 111 DNA molecules (B and D).

by a high-pressure water rinse or by using water instead of buffer, but neither of these measures was used because they both decrease the amount of DNA bound to the mica by an order of magnitude.

Histograms. The measured end-to-end distances of DNA molecules were converted to the percent of total DNA length, binned in 10% intervals, and graphed as histograms. Although there was considerable end-to-end aggregation of molecules, which is especially evident in Figure 2C, only the molecules within approximately 15% of the expected length were measured. The expected length was based on a spacing of 0.34 nm/bp, which is consistent with the lengths obtained for DNA in the AFM (Hansma et al., 1993a).

Electrophoretic Mobility Shift Assay. For all of the reactions (20 μL), the final concentrations were 5.0 μg/mL (7.5 μM bp) M400 DNA in 20 mM HEPES–KOH, pH 7.6, and 5 mM $MgCl_2$. Incubation of the DNA, with or without 5.5 μM MGT-6b, **2**, or tren, was for 15 min at room temperature (ca. 25 °C). At this time, 1.1 μL of 10% (w/v) glycerol, 0.1% (w/v) sodium dodecyl sulfate, and 0.1% (w/v) bromophenol blue loading buffer was added to each sample. Samples were separated electrophoretically through a 4% NuSieve 3:1 agarose gel in 89 mM Tris–borate and 1 mM EDTA, pH 8.0 (1× TBE) for 2 h at 3.2 V/cm. The gel was stained with a 0.5 μg/mL solution of ethidium bromide in deionized water for 30 min, destained for 30 min in deionized water, and photographed on a UV (302 nm) transilluminator with Polaroid type 667 film.

RESULTS

Ligand Binding to Kinetoplast DNA. Linear restriction fragments of a bent segment of kinetoplast DNA (kDNA) 219-bp long show a large number of highly curved and even circular molecules in both the electron microscope (Barcelo et al., 1991; Griffith et al., 1986) and the atomic force microscope (Hansma et al., 1993b) (Figure 2A). In the presence of distamycin (Griffith et al., 1986) (Figure 2C) or MGT-6b (Figure 2E), the curvature of the DNA is greatly reduced.

The degree of curvature observed in the AFM has been quantified in the histograms of Figure 2. For fully extended kDNA molecules, the measured end-to-end distance is equal to the length of the molecules, i.e., 100% of the length, which is calculated to be 74 nm on the basis of the spacing per base pair that was measured previously with the AFM (Hansma et al., 1993a). For molecules that are curved into a circle, the end-to-end distance is zero or 0% of the DNA length. Under the conditions used here, the kDNA molecules showed a variety of degrees of curvature (Figure 2A,B), with "C"-shaped molecules being most common. Griffith and co-workers (Griffith et al., 1986) have shown that the percentage of kDNA molecules scored as circles in the electron microscope can be increased by lowering the incubation temperature to 4 °C.

Distamycin straightened the molecules significantly; the mean end-to-end distance increased to 72% of the DNA length (Figure 2D). MGT-6b extended the kDNA even more to a mean end-to-end distance of 83% of the DNA length (Figure 2F). The molar ratio of ligand (distamycin or MGT-6b) to DNA base pairs was 1:7 in these experiments. Variation of the ratio of MGT-6b to DNA base pairs showed that there was no further extension of the molecules at a ratio of 1:3.5. As the ratio changed in the other direction, to 1 MGT-6b molecule/21 bp, the molecules were straightened less; at a ratio of 1 MGT-6b/63 bp, the DNA was roughly as curved as in the absence of MGT-6b. These results are similar to those obtained by Griffith and co-workers with distamycin binding (Griffith et al., 1986).

Ligand Binding to Normal DNA. When MGT-6b is bound to restriction fragments of ϕX-174 RF DNA, the molecules appear *more* curved in the AFM (H. Hansma, unpublished results). To investigate this result further, we used a 400-bp DNA that is used as a molecular weight standard (M400). Since M400 DNA is used as a molecular weight standard for gel electrophoresis, it does not have conformational anomalies such as inherent bends or curves that affect its electrophoretic mobility. In the *absence* of MGT-6b (Figure 3A,B), M400 DNA appears approximately as straight as kDNA in the presence of MGT-6b (Figure 2E,F). And in the presence of MGT-6b (Figure 3D), the histogram of end-to-end distances

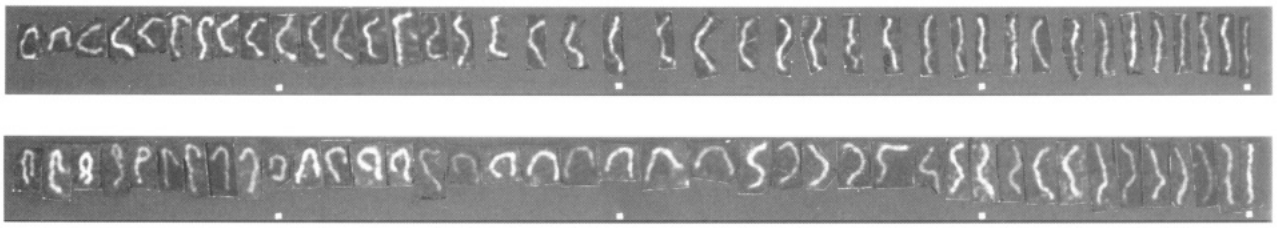

FIGURE 4: Forty molecules of M400 DNA, randomly selected, without (A, top) and with (B, bottom) MGT-6b at a concentration of 1 molecule MGT-6b/1.4 bp. Molecules are arranged in the order of decreasing bending. Dots mark tens of molecules.

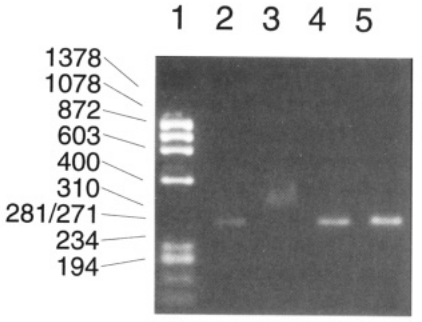

FIGURE 5: Electrophoretic mobility of M400 DNA in the absence (lane 2) and presence of 5.5 μM MGT-6b (lane 3), **2** (lane 4), and tren (lane 5) on a 4% agarose gel. The ratio of ligand molecules to DNA bp is 1:1.4. Lane 1 contains ϕX-174-RF DNA *Hae*III restriction digest fragments (sizes are indicated to the left side of the figure) as standards.

of M400 is quite similar to that of kDNA in the *absence* of MGT-6b (Figure 2B). The variety of molecular shapes can be seen from the arrays of 40 randomly selected molecules of M400 DNA without (Figure 4A) and with (Figure 4B) MGT-6b; the molecules in each group are arranged approximately in the order of the degree of curvature.

The results shown in Figures 2 and 3 are comparable to those obtained on different areas of the sample and those on different samples prepared from different incubations of DNA with ligand. Some areas of some samples show evidence of a flow-induced orientation similar to that in Figure 2E, but the degree of curvature seen in the molecules was independent of the degree of molecular orientation observed.

The M400 DNA molecules in Figures 3C,D and 4B were incubated at a molar ratio of 1 MGT-6b molecule/1.4 bp DNA. Less ligand gave less bending of the M400 DNA; there was little or no bending of M400 with 1 ligand molecule/7 bp DNA. Thus, the ligand-induced bending of M400 DNA occurs at higher ligand concentrations than the ligand-induced straightening of kDNA.

MGT-6b binding also causes a decrease in the electrophoretic mobility of M400 DNA to an apparent size larger than 400 bp and a broadening of the band on the gel, corresponding to sizes in the range of 470–580 bp (Figure 5, lane 3). The two pieces of which MGT-6b is composed, **2** and tren, do not alter the mobility of M400, which migrates normally at the position expected for 400-bp DNA (Figure 5).

The ligands **2** and tren do not bend M400 DNA, as seen through the AFM (H. Hansma, unpublished results). Thus, it appears that MGT-6b requires both parts of its "vise grip" to bend M400 DNA—both the polyamine that binds to the phosphate backbone and the tripyrrole that binds to the minor groove.

DISCUSSION

Effects of Ligand Binding on Electrophoretic Mobilities. The electrophoretic mobility of normal DNA is decreased by distamycin (He et al., 1994; Wu & Crothers, 1984) and decreased even more by MGT-6b (He et al., 1994) (Figure 5). DNA normally migrates through agarose at rates that are inversely proportional to the logarithm of the number of base pairs (Helling et al., 1974). Larger DNA fragments showed a greater decrease in migration at comparable ligand concentrations (He et al., 1993, 1994). Therefore, the decreased electrophoretic mobility was not due to a change in the charge-to-mass ratio. Instead, a change in DNA conformation after ligand binding was proposed, but in the absence of visual evidence, it was not known whether this was due to the stiffening, unwinding, physical lengthening, or bending of the DNA (He et al., 1993, 1994). The AFM images presented here provide direct visual proof that the ligand-induced decrease in the electrophoretic mobility of normal DNA is due to DNA bending.

Kinetoplast DNA, which is curved in the absence of ligand, also has a slow electrophoretic mobility, which can be increased by distamycin to the mobility expected for its size (Barcelo et al., 1991; Wu & Crothers, 1984). It has been proposed that the bent DNAs are retarded in gels because they have a larger effective diameter than the linear DNAs (Marini et al., 1982).

MGT-6b not only decreases the mobility of normal DNA such as M400 (Figure 5) but it also broadens the band, giving the appearance of a range of molecular weights. This is consistent with the histograms of Figure 3, which also show that the range of DNA conformations is broader in the presence of MGT-6b than in its absence.

Ligand Binding Sites. The preferred binding sites of MGT-6b on DNA have been determined by footprint analyses of MGT-6b bound to a 167-bp DNA fragment containing four runs of three A's. The molar ratios of MGT-6b in the footprint studies ranged from 0.05 to 1 molecule of MGT-6b/bp DNA (He et al., 1994). This analysis shows that MGT-6b, like distamycin (Harshman & Dervan, 1985; He et al., 1994; Mendoza et al., 1990) and its other analogs (Baker & Dervan, 1989), binds preferentially to runs of three or more A's (adenines) with a thymine or perhaps a cytosine at one end, as evidenced by the protection from DNase I cleavage at these sites.

Both 2D NMR and fluorescence studies indicate that two molecules of MGT-6b can bind to dsDNA containing the sequence, CAAATTTG (Blaskó et al., 1994; He et al., 1994). In the formation of DNA·L_2 complexes, the equilibrium constant for formation when L is MGT-6b is ca. 10^3 greater than when L is **2** (Browne et al., 1993; He et al., 1994).

Ligand Binding Sites and Bends in M400 DNA. M400 DNA has runs of three or four A's located at seven sites: three in the first 40% of the molecule, at positions 108, 141, and 162, and four in the last 30% of the molecule, at positions 287, 308, 336, and 390. As described above, footprint analyses show that MGT-6b binds selectively to runs of three or more A's (He et al., 1994). To investigate the relationship between runs of A's and bends in M400 DNA, we analyzed the positions

of the bends in M400 DNA molecules with bound MGT-6b. The most striking observation is the wide variety of molecular conformations of M400 DNA in the presence of MGT-6b (Figures 3 and 4). The second observation is that hairpin turns in M400 DNA molecules are seen only in the presence of MGT-6b.

Since M400 molecules with hairpin turns are seen in the presence of MGT-6b (first 11 molecules in Figure 4B) but not in the absence of MGT-6b (Figure 4A), the positions of these hairpin turns were compared with the positions of runs of A's, which should bind MGT-6b. Most of the hairpins were centered around two or three runs of A's, such as 141 and 162 (e.g., the sixth molecule in Figure 4B) or 287–336 (e.g., the ninth molecule in Figure 4B), but other hairpins are closer to the center of the molecule, being centered around only the run of A's at position 162 (e.g., the third molecule in Figure 4B). Diameters at the hairpin turns ranged from 14 to 26 nm, giving values of 130 to 240 bp for a complete circle. These are comparable to the length of the kDNA (219 bp), which forms circles with diameters of approximately 20 nm. In kDNA, bends of this magnitude can be attributed to 18 runs of A's occurring at a similar position in every helix turn (Kitchin et al., 1986), but with M400 DNA, similar bends seem to result from the binding of MGT-6b at only one to three runs of A's. Although these bends look sharp, DNA can also bend much more, since 200 bp of DNA can wind twice around a 5-nm nucleosome (Allen et al., 1993; Griffith, 1975).

Stoichiometries of Ligand Binding. The segment of kDNA used in these studies has 18 runs of four to six A's per 219-bp molecule (Kitchin et al., 1986), and these runs of A's are the preferred binding sites for distamycin (Harshman & Dervan, 1985; Mendoza et al., 1990) and MGT-6b (He et al., 1994). Ligand-induced straightening is observed with as little as 1 molecule of MGT-6b/21 bp kDNA, which corresponds to 0.6 MGT-6b molecule/run of A's; maximum straightening occurs with less than two molecules of MGT-6b/run of A's. Thus, very little MGT-6b is needed to produce conformational changes in kDNA.

In contrast, normal DNA (M400) needs much more MGT-6b for observable conformational changes. M400 DNA has only seven runs of three or more A's per molecule, which are known to be preferred binding sites for MGT-6b (He et al., 1994). Ligand-induced bending of M400 DNA is first observed with 16 molecules of MGT-6b/run of A's, and the bending in Figures 3C,D and 4B occurred with 40 molecules of MGT-6b/run of A's. These are similar to the stoichiometries needed for footprint analyses of the ligand binding sites on normal DNA: 20 ligand molecules/run of A's protected the DNA from nuclease digestion, while 2 ligand molecules/run of A's was not sufficient to protect the DNA. Footprint analyses also show that more bases are protected adjacent to runs of A's as the concentration of the ligand MGT-6b is increased to 100 ligand molecules/run of A's, but even at this high concentration, only about three to four additional base pairs are protected adjacent to the runs of A's (He et al., 1994).

CONCLUSION

The AFM's ability to visualize individual DNA molecules makes it a valuable tool for investigating DNA conformations at the molecular level. Using the AFM, we have obtained visual evidence that small organic ligands can bend DNA. We have shown that approximately 1 molecule of MGT-6b/run of A's can straighten kDNA, while tens of MGT-6b molecules per run of A's are needed to bend normal DNA. Similar amounts of MGT-6b are needed to protect runs of A's in normal DNA in footprint analyses (He et al., 1994), which supports the hypothesis that ligand-induced bending is due to ligand binding at runs of A's. We anticipate that the AFM will continue to be useful in visualizing the effects of ligand binding to DNA as the chemistry of these ligand molecules continues to evolve.

ACKNOWLEDGMENT

We thank Elliott Dawson of BioVentures for providing custom samples of M400 DNA and sequence information, Paul Englund for providing pPK201/CAT, Jay Groppe for isolating and purifying the kDNA fragment, Felice Chu Lightstone for information about DNA bending, Paul Hansma and Robert L. Sinsheimer for helpful discussions, and David Vie for untiring technical assistance.

REFERENCES

Allen, M. J., Dong, X.-F., O'Neill, T. E., Yau, P., Kowalczykowski, S. C., Gatewood, J., Balhorn, R., & Bradbury, E. M. (1993) *Biochemistry 32,* 8390–6.

Baker, B. F., & Dervan, P. B. (1989) *J. Am. Chem. Soc. 111,* 2700–2712.

Barcelo, F., Muzard, G., Mendoza, R., Revet, B., Roques, B. P., & LePecq, J. B. (1991) *Biochemistry 30,* 4863–73.

Binnig, G., Quate, C. F., & Gerber, C. (1986) *Phys. Rev. Lett. 56,* 930–933.

Blaskó, A., Browne, K. A., & Bruice, T. C. (1994) *J. Am. Chem. Soc. 116,* 3726–3737.

Browne, K. A., He, G.-X., & Bruice, T. C. (1993) *J. Am. Chem. Soc. 115,* 7072–7079.

Caddle, M. S., Dailey, L., & Heintz, N. H. (1990) *Mol. Cell. Biol. 10,* 6236–43.

Gille, H., Egan, J. B., Roth, A., & Messer, W. (1991) *Nucleic Acids Res 19,* 4167–72.

Griffith, J. D. (1975) *Science 187,* 1202–1203.

Griffith, J., Bleyman, M., Rauch, C. A., Kitchin, P. A., & Englund, P. T. (1986) *Cell 46,* 717–724.

Hansma, H. G., & Hansma, P. K. (1993) *Proc. SPIE—Int. Soc. Opt. Eng. 1891,* 66–70.

Hansma, H. G., & Hoh, J. (1994) *Annu. Rev. Biophys. Biomol. Struct.* in press.

Hansma, H. G., Vesenka, J., Siegerist, C., Kelderman, G., Morrett, H., Sinsheimer, R. L., Bustamante, C., Elings, V., & Hansma, P. K. (1992) *Science 256,* 1180–1184.

Hansma, H. G., Bezanilla, M., Zenhausern, F., Adrian, M., & Sinsheimer, R. L. (1993a) *Nucleic Acids Res. 21,* 505–512.

Hansma, H. G., Sinsheimer, R. L., Groppe, J., Bruice, T. C., Elings, V., Gurley, G., Bezanilla, M., Mastrangelo, I. A., Hough, P. V. C., & Hansma, P. K. (1993b) *Scanning 15,* 296–299.

Harshman, K. D., & Dervan, P. B. (1985) *Nucleic Acids Res. 13,* 4825.

He, G.-X., Browne, K. A., Groppe, J. C., Blaskó, A., Mei, H.-Y., & Bruice, T. C. (1993) *J. Am. Chem. Soc. 115,* 7061–7071.

He, G.-X., Browne, K. A., Blaskó, A., & Bruice, T. C. (1994) *J. Am. Chem. Soc. 116,* 3716–3725.

Helling, R. B., Goodman, H. M., & Boyer, H. W. (1974) *J. Virol. 14,* 1235–1244.

Kitchin, P. A., Klein, V. A., Ryan, K. A., Gann, K. L., Rauch, C. A., Kang, D. S., Wells, R. D., & Englund, P. T. (1986) *J. Biol. Chem. 261,* 11302–11309.

Marini, J. C., Levene, S. D., Crothers, D. M., & Englund, P. T. (1982) *Proc. Natl. Acad. Sci. U.S.A. 79,* 7664–7668.

Mendoza, R., Markovits, J., Jaffrezou, J.-P., Muzard, G., & LePecq, J.-B. (1990) *Biochemistry 29,* 5035–5043.

Perez-Martin, J., & Espinosa, M. (1993) *Science 260,* 805–807.

Rees, W. A., Keller, R. W., Vesenka, J. P., Yang, C., & Bustamante, C. (1993) *Science 260,* 1646–1649.

Rugar, D., & Hansma, P. K. (1990) *Phys. Today 43,* 23–30.
Shi, Q., Thresher, R., Sancar, A., & Griffith, J. (1992) *J. Mol. Biol. 226,* 425–32.
Spolar, R. S., & Record, M. T. (1994) *Science 263,* 777–784.
Vesenka, J., Guthold, M., Tang, C. L., Keller, D., Delaine, E., & Bustamante, C. (1992) *Ultramicroscopy 42–44,* 1243–1249.
vonHippel, P. H. (1994) *Science 263,* 769–770.
Wade, S. W., & Dervan, P. B. (1987) *J. Am. Chem. Soc. 109,* 1574.
Wu, H.-M., & Crothers, D. M. (1984) *Nature 308,* 509–513.
Zhong, Q., Inniss, D., Kjoller, K., & Elings, V. B. (1993) *Surf. Sci. Lett. 290,* L888–L692.